Parametric Numerical Study of Off-Axis Pulse Tube Losses

T.I. Mulcahey[1], R.P. Taylor[2], S.M. Ghiaasiaan[1], C.S. Kirkconnell[3], M.G. Pathak[1]

[1] Georgia Tech Cryo Lab, Georgia Institute of Technology
Atlanta, GA 30332

[2] Virginia Military Institute
Lexington, VA 24450

[3] Iris Technology Corporation
Irvine, CA 92614

ABSTRACT

Recently there has been an emphasis on applying numerical modeling, with varying degrees of complexity, to the study of the notorious sensitivity of the pulse tube cryocooler to off-axis operation. Previous work has demonstrated the suitability of applying multi-dimensional CFD simulation to the pulse tube cryocooler both as a whole and at the component level for qualitative and quantitative analysis of system performance and losses. To date there has been no comprehensive study of the pulse tube losses for a wide range of operating conditions consistent with modern coolers currently used in both the military and civilian sectors. This work presents for the first time a comprehensive loss analysis of the linear pulse tube cryocooler operating at common conditions using full three-dimensional CFD coupled with a real gas model for the working fluid.

The scope of results presented includes both system level models and a pulse tube/heat exchanger component level model. Results from the system level simulations are presented for two pulse tube aspect ratios at tilt angles of 0°, 91°, and 135°. Component level simulation results are presented and discussed for permutations in tilt angle between 0-180°, length-to-diameter aspect ratios from 4-8, cold tip temperatures from 4-80 K, phase angles between -30° and +30°, and an operating frequency range of 25-60 Hz. The entire set of modeling results is compiled and used to show a correlation between the normalized pulse tube cryocooler losses as a function of a non-dimensional pulse tube number. Discussion is also provided regarding the utility of component level simulation compared to system level simulation considering analysis complexity, computational resource requirements, and suitability for cooler design.

INTRODUCTION

Effective and efficient operation of pulse tube cryocoolers requires thermal stratification of the gas column within the pulse tube component. Many pulse tube coolers experience a reduction or elimination of cooling performance when operating in orientations other than cold end down,

Cryocoolers 18, edited by S.D. Miller and R.G. Ross, Jr.

which often leads to convective instability [1]. Previous publications have shown that the operating conditions and pulse tube geometry have a marked effect on off-axis sensitivity, but a consistent set of design standards has yet to be defined which minimize this sensitivity [2]. An exhaustive experimental study to characterize the relationships between the parameters responsible for convective losses is limited by the difficulty associated with making direct measurements in an operating cryocooler without disturbing the flow. Previous studies have been performed at elevated temperatures, typically with a substitute working gas such as dry air in place of the pressurized helium used in modern pulse tubes.

As a substitute for experimentation, modeling of the pulse tube flow and thermal physics using computational fluid dynamics (CFD) packages has been used as a predictive tool [3,4]. Previous publications have disclosed an experimentally validated 3-D half-symmetric CFD implementation which can effectively simulate and predict the parasitic losses [5-7]. The currently reported study discusses the implementation of this CFD methodology in a broad parametric study carried out using cluster computing resources to simulate a wide range of working conditions. The results of these simulations are used to compute non-dimensional losses and pulse tube convection numbers N_{PTC} as a function of the driving parameters.

PULSE TUBE THERMODYNAMICS AND CONVECTIVE INSTABILITY

Simulation of the pulse tube requires a clear understanding of the energy flows, real and theoretical, specific to this component. The relevant energy flows, and their directions, are noted in Figure 1 and consistent with a cycle-averaged condition. In Figure 1, boundary planes one (1) and two (2) represent the cold and warm ends, respectively.

Pulse Tube Thermodynamics

Thermodynamically, the pulse tube converts the Gibbs free energy to an enthalpy flow (travels from cold to warm). The Gibbs energy is often referred as the acoustic (PV) power and is expressed as,

$$\left\langle P\dot{V}\right\rangle = \frac{1}{2} P_d \dot{V}_d \cos\left(\theta_{m-p}\right) \tag{1}$$

where P_d is the dynamic pressure amplitude, V_d is the volume flow amplitude, and $\theta_{m\text{-}p}$ is the phase between mass flow and pressure. In an ideal pulse tube, the conversion is perfect and the enthalpy flow is equal to the Gibbs energy. Using this idea, coupled with the remaining terms in Figure 1, the total net energy flow in the pulse tube at a cyclic condition is,

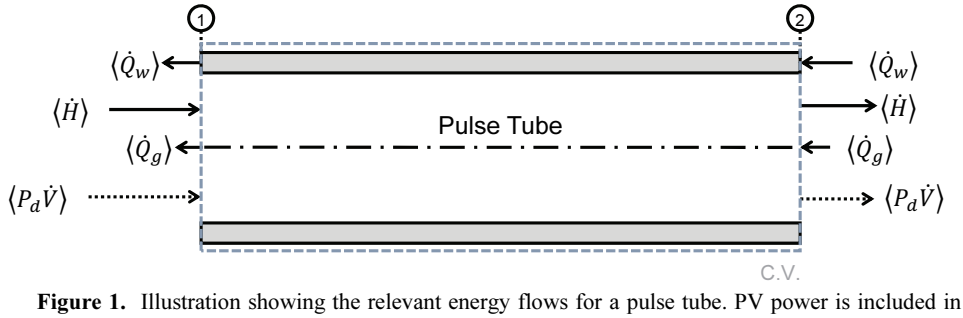

Figure 1. Illustration showing the relevant energy flows for a pulse tube. PV power is included in the energy flow diagram with dashed arrows for reference. The temperature gradient is cold to hot from left to right, i.e. from 1→2.

$$\left\langle \dot{E}_{PT,net} \right\rangle = \left\langle \dot{H} \right\rangle - \left\langle \dot{Q}_g \right\rangle - \left\langle \dot{Q}_w \right\rangle \tag{2}$$

where $\left\langle \dot{H} \right\rangle$ is the pulse tube enthalpy flow, $\langle \dot{Q}_g \rangle$ is the conduction in the working fluid, and $\left\langle \dot{Q}_w \right\rangle$ is the conduction in the solid wall of the pulse tube. In practice, the acoustic power to enthalpy conversion is not perfect due to numerous complex loss mechanisms that include all forms of streaming, shuttle heat transport, turbulent mixing and jetting, and gravitationally induced instability. All these mechanisms reduce the available enthalpy flow in the pulse tube and subsequently the cooling power. Minimizing these losses has been the subject of numerous empirical and numerical studies over the years. However, the physical mechanisms of these losses are generally well understood with the exception of gravitationally-induced instability.

The gravitationally-induced stability loss in pulse tube coolers is the single largest drawback to adoption for many applications. This is due to severe cooling power degradation when operated in a configuration where the temperature gradient (cold below warm) is not aligned with the gravitational field. As the cooler deviates from the ideal gradient orientation with respect to gravity, the flow becomes unstable and a buoyant circulation cell develops. Compounding this specific loss is the high degree of sensitivity witnessed with respect to geometry, mass flow amplitude, and driving frequency. In this work, we quantify this loss as,

$$\left| L(\theta) \right| = \frac{\left\langle \dot{E}_{PT,net}(0) \right\rangle - \left\langle \dot{E}_{PT,net}(\theta) \right\rangle}{\left\langle \dot{E}_{PT,net}(0) \right\rangle} \tag{3}$$

where $\left\langle \dot{E}_{PT,net}(0) \right\rangle$ is the net pulse tube energy flow at zero degrees deviation from ideal and $\left\langle \dot{E}_{PT,net}(\theta) \right\rangle$ is the net pulse tube energy flow at an angle removed from zero. A clear understanding of this loss is required to enable use of modern high-frequency pulse tube coolers in applications where the ideal cooler-gravitation alignment is unrealistic.

Convective Instability

A classic example of convective instability arises in an enclosure in which the top and bottom surfaces are at differing temperatures and the vertical surfaces are adiabatic. At some critical temperature differential, the buoyant forces in the fluid overcome viscous forces and free convection cells develop. The strength of these cells is proportional to the magnitude of the imbalance in forces and is characterized using the Rayleigh number. In many ways, a pulse tube is very similar, but also markedly different. In the pulse tube, unlike the case mentioned above, there is a non-zero bulk velocity arising from the oscillating flow field. In this combined scenario, the convection stability criteria can be related to a ratio of the inertial forces in the oscillating fluid relative to the buoyant forces in the fluid. Due to the high degree of non-linearity in the governing hydrodynamic, thermal, and state equations, closed-form solutions of this phenomenon are intractable. As a result, semi-empirical solutions based on analogous dynamic systems are used.

Recent work by Swift and Backhaus [8, 9] has likened the convective instability in pulse tubes to that of an inverted pendulum. This analogy is interesting as a statically unbalanced inverted pendulum can be dynamically stabilized using correct dynamic excitation at the base. This tracks with experimental observation of modern high frequency pulse tube cooler system. It has been noted that increased operating frequency lends to off-axis convective stability resulting in minimal losses. Empirical work by Swift and Backhaus resulted in development of a non-dimensional pulse tube convection number expressed as,

$$N_{PTC} = \frac{\omega^2 a^2}{g\left(\alpha_s D \sin\theta - L\cos\theta\right)} \sqrt{\left(\frac{\Delta T}{T_{avg}}\right)} \tag{4}$$

where ω is the angular frequency, a is the mass flow amplitude, g is gravitational acceleration, α_s is empirical fitting parameter, D is the pulse tube diameter, L is the pulse tube

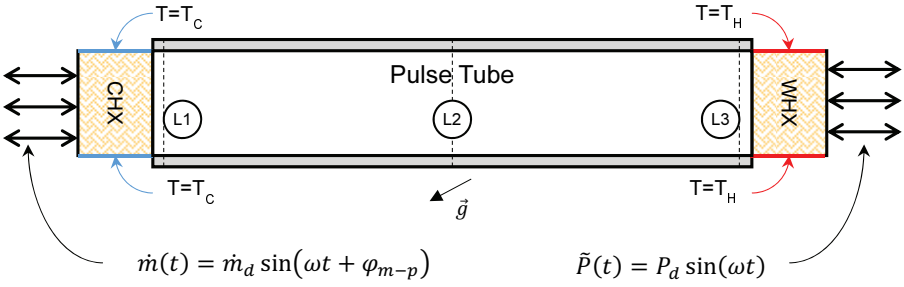

Figure 2. Schematic view of the computational domain along the plane of symmetry. Patterned sections represent porous domains. Solid filled wall section represents solid domain. Dashed lines represent computational monitor planes. Double headed arrows represent oscillatory boundary conditions.

length, θ is the angle from vertical, ΔT is the temperature difference between hot and cold, and T_{avg} is the average gas temperature in the pulse tube. This non-dimensional parameter stems from a force balance on the cold-warm gas system and the reader is referred to [8] for the full mathematical derivation. To date, this parameter has shown some validity but is insufficient in predicting correct criteria for minimizing the convective instability present in pulse tubes. This is attributed to numerous underlying assumption ranging from buoyancy being simplified to application of the Boussinesq approximation to slender pulse tubes. Due to the clear difficulty in developing pulse tube convective stability criteria using low order models, relaxation of simplifying assumptions is required. This requirement lends to use of high-order computational models with the primary drawback arising from orders of magnitude increase in solution time.

SIMULATION METHODS

A brief overview of the key characteristics of the ANSYS CFD [10] simulation methods used in this study will be given here. For explicit details of the simulation methods the reader is directed to the detailed disclosure given in [5], which describes two distinct methods for simulating the convective losses: a full-system approach which explicitly simulates all pulse tube cooler components, and an isolated model that includes only the pulse tube and adjacent heat exchangers. All simulations are performed in 3-D half-symmetry, with the symmetry plane coincident with the plane in which the gravity vector varies. It has been shown an isolated model introduces approximately 6% error to the predictions, while reducing the number of CPU's required for parallel processing from 64 to 12 and simultaneously reducing the simulation time from 32 days down to 12 days. Validation of this model against a set of commercial cryocoolers is given in [6], where error was reported as a percentage of the net energy flow across the pulse tube. An average error of 3.7% and a maximum error of 8.2% were reported using this modeling methodology, with largest errors occurring when the cooler was driven below its design input power, resulting in very low Reynolds numbers and therefore was most unstable. Numerical simulation error magnitudes were in the range of approximately 100 mW, indicating that the simulation method is most aptly suited for pulse tube coolers with larger net cooling capacity.

An open system modeling method is used to model the isolated domain consisting of the cold heat exchange (CHX), pulse tube, and warm heat exchanger (WHX) as shown in Figure 2. A sinusoidal mass flow condition with specified temperature, magnitude and phase angle relative to pressure oscillation is applied at the entrance to the CHX. A sinusoidal pressure with specified amplitude and frequency ω provides closure to the fluid domain at the warm heat exchangers. Isothermal boundary conditions at the cold and warm heat exchangers allow energy to flow in and out of the domain. Monitoring surfaces are defined across the pulse tube, denoted L1, L2 and L3, which record the thermodynamic and hydrodynamic parameters required to compute and isolate energy flows across the domain. Conjugate heat transfer with the pulse tube wall is

included to simulate thermally driven boundary phenomena that may impact off-axis performance. Gas properties are referenced to the NIST real gas models reported in the REFPROP database [11]. The heat exchangers are modeled as porous domains with hydrodynamic parameters consistent with those reported for packed screens in oscillatory flow [12].

The domain is spatially discretized using approximately 75,000 ordered mesh elements, the minimum quantity found to yield grid-independence with discretization error less than 0.5% of the net pulse tube energy flow. Inflation meshing was used within the fluid domain to capture boundary effects. The transient simulation was carried out to periodic steady state using time steps that yielded 400 samples per period of oscillation. Typical simulations required approximately 30,000 time steps for the solution to converge for convectively stable configurations. Simulations were carried out on high performance computing (HPC) cluster resources in order to compute the solution in 12 parallel processes, with a simulation duration of approximately 255 hours per case. In some instances 24 CPUs were used for each case, which reduced simulation time to 155 hours.

RESULTS

This study examines the results of 120 simulated pulse tube conditions with driving frequency ranging from 25 Hz to 60 Hz, cold end temperatures from 4 K to 80 K, rejection temperatures of 20 K to 300 K, mass flow rates from 1 g/s to 4 g/s, and mass flow phase angles of -30° to +30° relative to pressure. Two computational domains were used with length/diameter

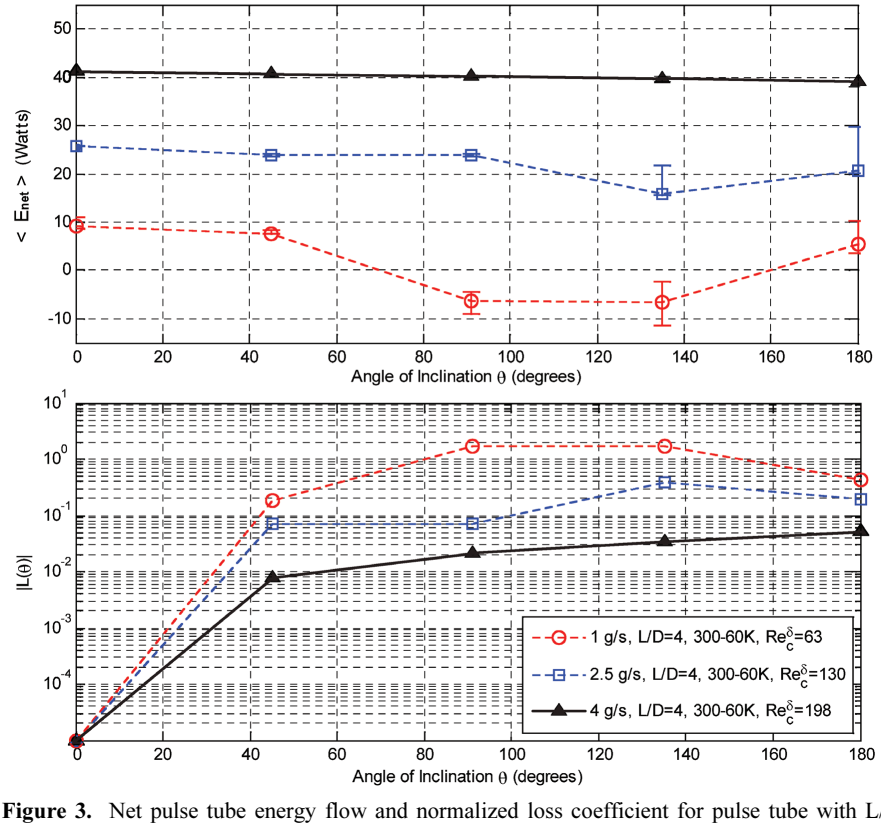

Figure 3. Net pulse tube energy flow and normalized loss coefficient for pulse tube with L/D=4 aspect ratio driven at 60 Hz at various mass flows in five discrete orientations with respect to gravity. Phase angle of -30° (mass lags pressure) and pressure ratio of 1.2 operating between 300 K and 60 K.

aspect ratio of eight (8), commonly used as a design minimum, and four (4), which is often required for larger capacity pulse tubes as cross-sectional area scales with mass flow while length does not. Experimentally measured off-axis performance for three commercial cryocoolers are also included in the analysis to add to the body of data from which to draw conclusions.

Upon completion, each simulation was post-processed to determine the net energy flow defined in Equation 1 across the pulse tube at the cold end, adjacent to the cold heat exchanger but within the gas domain outside the transition from porous to open flow channel. The energy flow data at varying inclination angle θ was compared to the energy flow in the vertical orientation via Equation 3, yielding the normalized energy flow loss |E|, for which a value of zero indicates no reduction in cooling performance at the specified angle, a value of one indicates complete loss of net cooling power, and a value greater than one indicates that the pulse tube acts as a parasitic heat pipe and transfers energy from the warm end to the cold end, resulting in heating. Normalized energy flow loss is plotted in Figures 3 and 4 to indicate the order of magnitude reduction in sensitivity resulting from changes in the oscillatory Reynolds number Re^{δ} [13]. The Reynolds number based on Stokes' boundary layer thickness is used to characterize the flow and ranges from 43 (very laminar) to 350, where the transition to intermittent turbulence is approximately 500.

Figure 3 gives representative energy flow loss data as a function of the mass flow amplitude, and therefore the Reynolds number, for a pulse tube with length-to-diameter aspect ratio of four (4) under the typical pulse tube design condition that mass flow lags pressure by 30°. The average pressure used in all simulations was 2.0 MPa with a pressure amplitude of 400 kPa. The

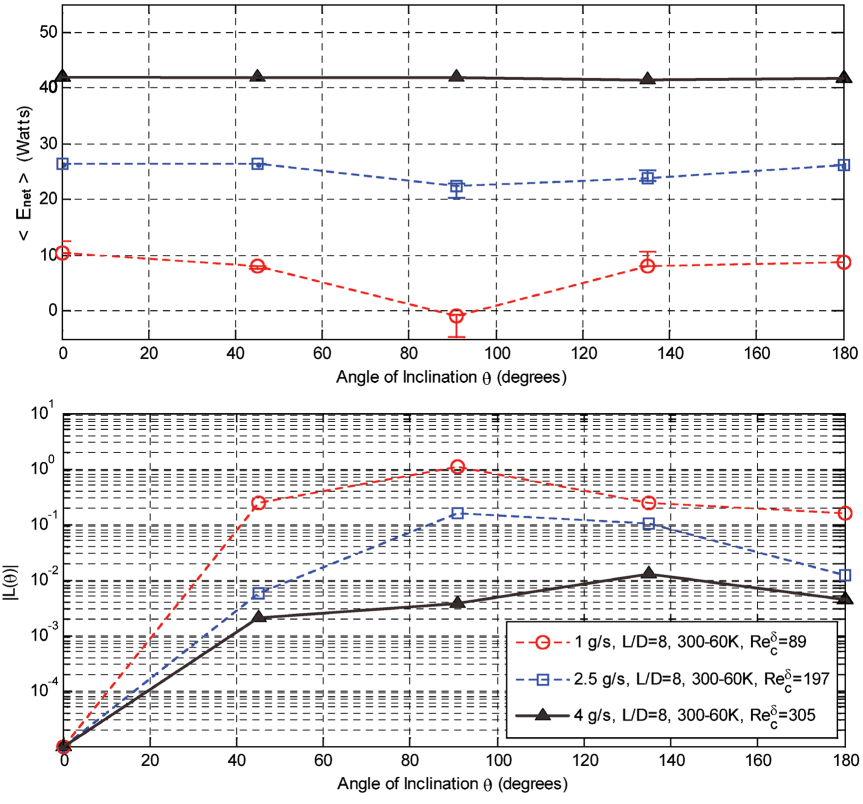

Figure 4. Net pulse tube energy flow and normalized loss coefficient for pulse tube with L/D=8 aspect ratio driven at 60 Hz at various mass flows in five discrete orientations with respect to gravity. Phase angle of -30° (mass lags pressure) and pressure ratio of 1.2 operating between 300 K and 60 K.

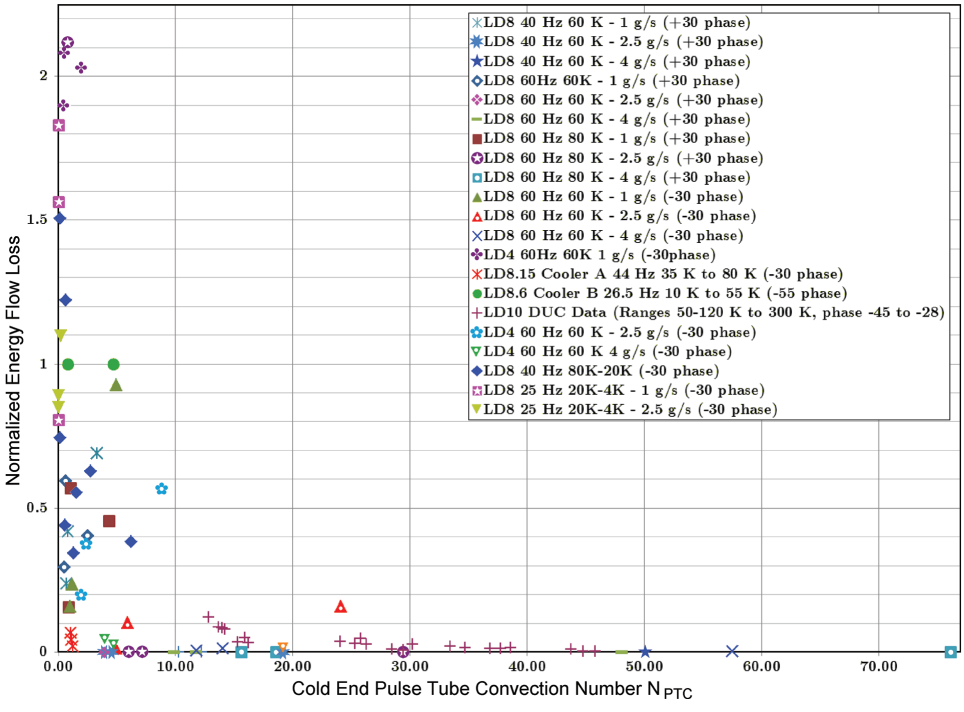

Figure 5. |L| vs NPTC results. Legend entries indicate the aspect ratio (LD), driving frequency, cold end temperature, mass flow, and phase angle of mass flow relative to pressure.

mass flow amplitude is directly related to the input power, and therefore the efficiency decreases significantly for higher mass flows at inclination angles above 45°. The error bars displayed in the net energy flow plots in Figures 3 and 4 are used for unstable cases to show the maximum and minimum energy flows observed over the final 0.25 s of simulated flow time. Larger error bars indicate a more unstable flow regime.

Figure 4 compares performance for a pulse tube with identical operating conditions to the results reported in Figure 3 and identical pulse tube gas volume but stretched to an aspect ratio of eight (8). In this case, only a single operating point (1 g/s, 90° orientation) resulted in catastrophic loss of cooling, and an increase in the mass flow rate to 4 g/s reduced orientation sensitivity by two orders of magnitude.

In order to assimilate all data sets collected, the pulse tube convection number N_{PTC} defined by Equation 4 was computed for each case. Figure 5 compares the normalized energy flow loss |L| to the computed pulse tube convection number N_{PTC} for all data collected in this study, both numerically simulated and experimentally measured. A key characteristic of the plot in Figure 5 is the notable scatter in sensitivity throughout the range of N_{PTC}. This suggests that the pulse tube convection number can be used as an order of magnitude indication of the orientation sensitivity, but not to directly compute the expected change in energy flow.

Figure 6 shows example temperature contours and velocity vectors for the vertical and unstable off-axis operation for the same physical design and operating parameters. The cross-sectional temperature variation shown in Figure 6d illustrates the need to use 3-D modeling techniques that would not be accounted for with a 2-D simulation strategy.

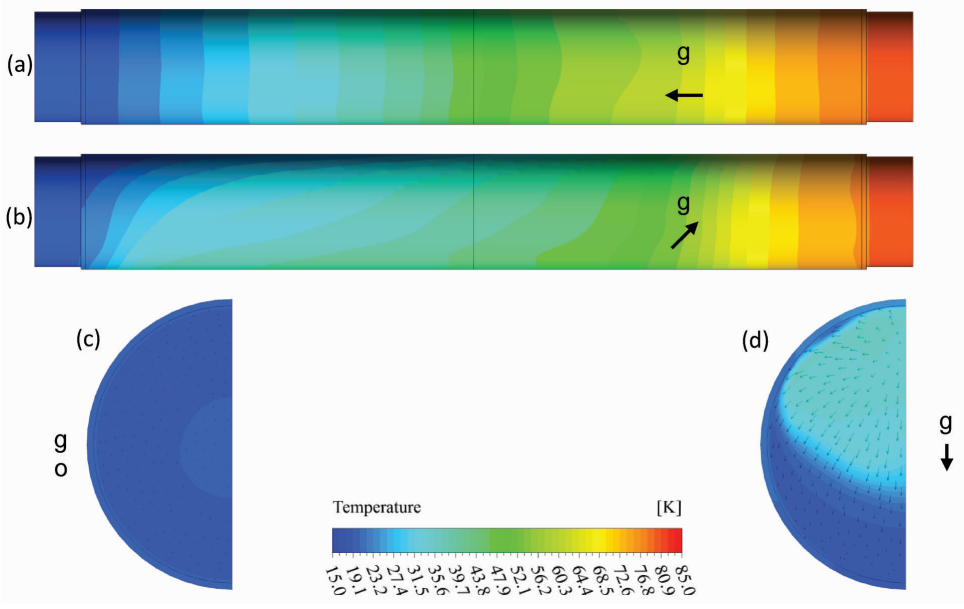

Figure 6. Sample temperature contours comparing stable (a,c) and unstable (b,d) operation for a 40 Hz pulse tube operating between 80 K and 20 K. **(a)** 0° orientation view of pulse tube exterior wall. **(b)** 135° orientation view of pulse tube exterior wall. **(c)** cross-section view of temperature contours and velocity vectors at the cold end for 0° orientation. **(d)** cross-section view of temperature contours and velocity vectors at the cold end for 135°orientation. Note that velocity vectors in (d) illustrate the 3-D nature of the convection problem at hand.

DISCUSSION

In general, observation of the data presented in Figure 5 yields interesting trends. There is notable evidence that use of higher operating frequency, when possible, is advisable. Furthermore, larger aspect ratio pulse tubes generally perform better off-axis for temperatures above ~60K. For temperatures below ~15K, off-axis effects are noticeably more severe as expected due to the larger disparity in density between cold and warm when compared to more moderate temperature cases. Finally, larger mass flow amplitudes generally serve to reduce the off-axis sensitivity. This is attributed to larger inertial forces, which are stabilizing when compared to the buoyancy forces.

All of the observed cases reported in Figure 5 report orientation sensitivity in terms of normalized energy flow loss below a bounding function which is fitted to the largest observed loss over the full range studied. These extreme points are fitted with an exponential decay function of the form shown in Equation 5. All points simulated and measured fall below the cutoff line described by Equation 5.

$$|L(\theta)|_{max} \leq 2.5014e^{-0.114N_{PTC}} \tag{5}$$

The utility of the data reported herein is the ability to determine the expected order of magnitude loss as a function of a calculated pulse tube convection number for a given theoretical design. This factor can be incorporated in a scoping level study to avoid designs that indicate undesirable orientation sensitivity. Once a prospective design is developed, it should be examined using the above described 3-D CFD methodology at the worst anticipated angle of inclination to verify the level of sensitivity prior to fabrication.

CONCLUSION

Three-dimensional CFD simulation has been successfully applied to predict the performance losses due to gravity-driven convective instability in pulse tube cryocoolers over a wide range of operating characteristics and two geometries. The results were characterized in terms of a nondimensional loss of net energy flow as well as the non-dimensional pulse tube convection number. The results indicate that the magnitude of cooling power loss decays exponentially with increasing pulse tube convection number and sensitivity is minimized by applying the design which yields the highest laminar Reynolds number in the pulse tube. The reported relationship in this article should be used for scoping purposes only. Completed thermodynamic designs should be simulated in 3-D half-symmetry using the method described in [5] prior to implementation into hardware.

REFERENCES

1. Ross, R.G., and Johnson, D.L., "Effect of gravity orientation on the thermal performance of Stirling-type pulse tube cryocoolers," *Cryogenics*, vol. 44 (2004), pp. 403-408.
2. Berryhill, A. and Spoor, P.S., "High-frequency pulse tubes can't always be tipped," *Advances in Cryogenic Engineering*, vol. 1434 (2012), American Institute of Physics, pp. 1593-1599.
3. Taylor, R.P., "Development and Experimental Validation of a Pulse-Tube Design Tool Using Computational Fluid Dynamics," PhD thesis, The University of Wisconsin-Madison, 2009.
4. Taylor, R.P., Nellis, G. F., and Klein, S. A., "Optimal pulse tube design using computational fluid dynamics," *Advances in Cryogenic Engineering*, vol. 53B (2007), American Institute of Physics, pp. 1445-1451.
5. Mulcahey, T.I., *Convective Instability of Oscillatory Flow in Pulse Tube Cryocoolers due to Asymmetric Gravitational Body Force*, PhD thesis, Georgia Institute of Technology, 2014.
6. Mulcahey, T.I., Conrad, T.J., Ghiaasiaan, S.M., and Pathak, M.G., "Investigation of gravitational effects in pulse tube cryocoolers using 3-D CFD," *Advances in Cryogenic Engineering*, vol. 59 (2013), American Institute of Physics, pp. 1002-1009.
7. Mulcahey, T. I., Conrad, T. J., and Ghiaasiaan, S. M., "CFD modeling of tilt induced cooling losses in inertance tube pulse tube cryocoolers,"*Cryocoolers 17*, ICC Press, Boulder, CO (2012), pp. 143-150.
8. Swift, G.W. and Backhaus, S., "The pulse tube and the pendulum," *Journal of the Acoustical Society of America*, vol. 126, no. 5 (2009), pp. 2273-2284.
9. Swift, G.W. and Backhaus, S., "Why high-frequency pulse tubes can be tipped," *Cryocoolers 16*, ICC Press, Boulder, CO (2011), pp. 183-192.
10. ANSYS, ANSYS FLUENT User's Guide. No. Release 14.5, Canonsburg, PA 15317: Southpointe, 2012.
11. Lemmon, E.W. and Huber, M.L., REFPROP: NIST Materials Reference Properties Database: Version 9.1. NIST, 2013.
12. Cha, J.S., Ghiaasiaan, S.M., and Kirkconnell, C.S., "Measurement of anisotropic hydrodynamic parameters of pulse tube or Stirling cryocooler regenerators," *Advances in Cryogenic Engineering,* Vol. 51, Amer. Institute of Physics, Melville, NY (2006), pp. 1911-1918.
13. Akhavan, R., Kamm, R. D., and Shapiro, A. H., "An investigation of transition to turbulence in bounded oscillatory stokes flows: part 1. experiments," *J. Fluid Mechanics*, vol. 225 (1991), pp. 395-422.